Pergamon

Cement and Concrete Research, Vol. 25, No. 3, pp. 485-490, 1995

0008-8846/95 $9.50+.00

0008-8846(95)00036-4

THE MICROSTRUCTURE OF CONCRETE CURED AT ELEVATED TEMPERATURES

H H Patel, C H Bland and A B Poole
Geomaterials Unit
Queen Mary and Westfield College
London University
Mile End Road, London E1 4NS

(Communicated by A. Neville)
(Received November 10, 1994)

ABSTRACT

The temperature and relative humidity pertaining during curing influence the strength development, microstructure, and long term durability of concrete. Optical and electron microscopy techniques have been used to assess the microstructural characteristics of laboratory prepared concrete and case study material cured under a range of temperature and humidity regimes. Microstructural examination of two month old concrete cured at 16°C, 42°C and 46°C has revealed no marked differences in the spatial distribution, morphology, and volume of hydrates and other microstructural features present. A network of microcracks was evident within the matrix of all the concretes, with that cured at 85°C, and the sample with eighteen years in-service use, showing a higher degree of microcracking. The concretes prepared at temperatures above 46°C were also found to have significant development of hydrates, particularly ettringite, within pores and microcracks, together with a generally coarser microstructure.

INTRODUCTION

Within the precast concrete industry the use of elevated temperature curing techniques to accelerate early strength development has been adopted as one of the standard methods for high volume production of concrete units. However, research has shown that such curing leads to the development of a modified microstructure which has been associated with the phenomenon of secondary ettringite formation. Mature pastes cured at temperatures of between 50°C and 70°C have been reported to exhibit a coarser C-S-H morphology and pore structure than that characteristic of pastes cured under ambient conditions (1,2,3). The width of the C-S-H shell around hydrating cement grains was observed to increase with increasing cure temperature (4), while inner C-S-H in a paste cured at 80°C was reported to be denser than the outer hydrate (5). At elevated temperatures a greater proportion of portlandite was found to form dense clusters as opposed to the more usual lamellar-type morphology observed under ambient conditions (4). Recent work indicates a growing concern that, after long term exposure (particularly in moist conditions), concrete cured at elevated temperatures may show abnormal expansion and associated microcracking, which may lead to failure (6-12). In most of these studies either the alkali aggregate reaction or delayed ettringite formation, or both, was identified as the probable cause of the expansion.

EXPERIMENTAL PROGRAMME

The manufacturing details of the samples are summarised in Table 1. The concrete prisms were prepared under laboratory conditions using an OPC (3.5% C_3A) with a plasticiser and an air-entraining agent. The aggregate consisted of Mount Sorrel granite coarse (max. 20mm) and natural quartz sand fines. These samples were sealed in watertight containers, placed in a water bath to achieve the desired cure cycle (13), and were subsequently stored in water at 20°C. The concrete cubes were manufactured and cured under typical precast concrete production conditions using either free steam or captive steam to obtain a specific cure cycle, together with a control sample cured at 16°C under laboratory conditions. A RHPC (7.0% C_3A) was used with no air entraining agent, coarse aggregate (max. 20mm) largely consisting of granite with some limestone and minor quantities of quartzite, and a sand fraction dominated by quartz with some limestone; the cubes were stored subsequent to cure for two months in water at room temperature. A schematic outline of the cure cycles to which the concretes were subjected is given in Figure 1.

TABLE 1
Manufacturing Details of the Samples

Sample	Curing Regime						A/C	W/C
	P (hrs)	P (°C)	HR (°C/hr)	CT (°C)	T_{max} (hrs)	CR (°C/hr)		
A: Precast factory cubes				16			4.7	0.45
B: Precast factory cubes (FS)	7	16	6.5	42	12	6.5	4.7	0.45
C: Precast factory cubes (CS)	7	16	7.5	46	14	7.5	4.7	0.45
D: Laboratory prisms				20			3.8	0.45
E: Laboratory prisms	4	20	13	85	6	5.8	3.8	0.45

P : Precure time and temperature
HR : Heating rate
CR : Cooling rate
CT : Constant temperature
T_{max} : Time at maximum temperature
A/C : Aggregate/cement ratio

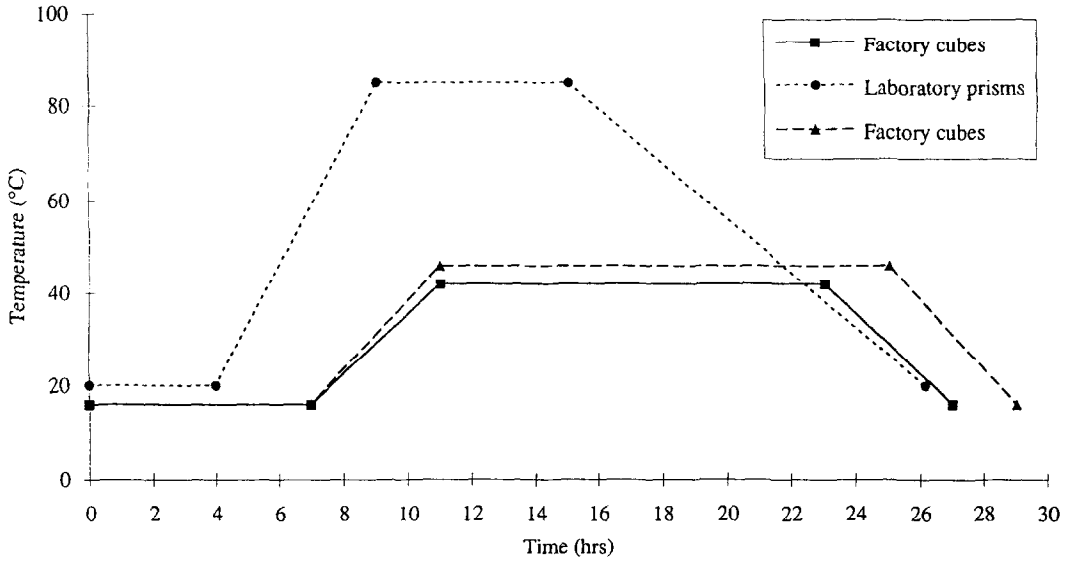

FIGURE 1
Temperature Profile of Concrete Samples During Curing

Samples were also obtained from precast concrete units with over eighteen years in-service use. While there is no available information on the history of these concretes, it can be assumed that the elevated temperature curing would have been typical of practise at their time of manufacture. Examination of the concrete has revealed the cement to be a Portland cement, with no air-entraining agent used. The aggregate consisted of a limestone coarse fraction and mixed fines containing quartz, shell fragments and some chert (indicative of sea-dredged origin).

Examination and analysis of the samples was carried out utilising both optical and electron microscopic techniques. Electron microscopy was employed to provide detailed information regarding the crystal form of hydrates, and the features associated with the paste/aggregate interface and microcracks, while transmitted light microscopy allowed hydrate phases and their crystal size to be identified more readily. Crystal type can be identified by electron microscopic examination of polished surfaces, although it can be difficult to ascertain whether the area identified represents one large crystal or a number of small ones; optical microscopy allows this distinction to be made, and thus an integrated approach to microstructural investigation was used. Gold coated fracture surfaces of concrete were examined using a Hitachi S450 scanning electron microscope fitted with an Oxford Instruments AN 10,000 microanalytical system, while more quantitative analysis was carried out on carbon coated polished surfaces. The latter were prepared by oven drying prior to resin impregnation and polishing on diamond laps to 0.25μm. A Carl Zeiss Jena 30-G0060a Polarising Research microscope was used for optical examination of standard petrographic thin sections 30μm thick impregnated with a blue resin.

RESULTS AND DISCUSSION

The relative size, distribution and abundance of residual clinker grains, various cement hydrates, and microcracks were assessed and the results are discussed in terms of their relationship to each other and to the curing regime. However, it should be emphasised that the concretes discussed here have different mix designs and have experienced differing curing and storage regimes; the effect of these factors on the microstructural development is not fully understood.

Residual clinker

Sample D showed a high degree of hydration, the result of extended water storage, characterised by the relative scarcity of residual clinker grains, while sample A showed more abundant residual clinker grains indicative of a lower degree of hydration. Samples B and C appeared very similar to those cured under ambient conditions, while sample E and the in-service concrete (F) both

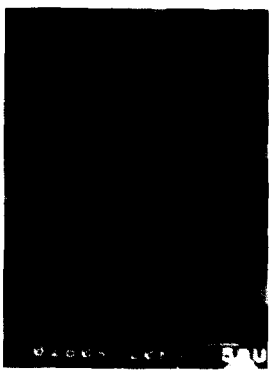

PLATE 1
Sample B: Backscattered electron image

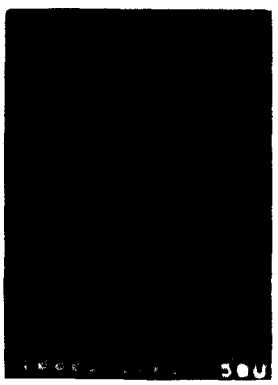

PLATE 2
Sample E: Backscattered electron image

revealed limited residual clinker compatible with their age and hydration histories (Plates 1-3). The concretes cured at elevated temperatures (B, C, E & F) showed some development of hollow shells, particularly close to the largest aggregate particles, the result of the complete hydration of clinker grains and the migration of ions away from the site of hydration (Plate 3).

PLATE 3
Sample F: Backscattered electron image

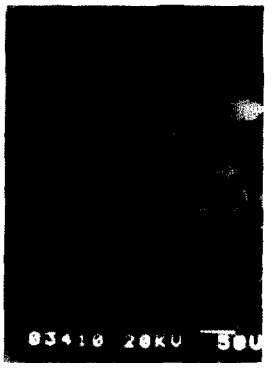

PLATE 4
Sample E: Optical micrograph (oblique polars, x30)

Cement hydrates

Portlandite (calcium hydroxide) was present in abundance in each of the concretes examined, being readily identifiable by both optical and electron microscopy. Irrespective of curing temperature, the morphology and spatial distribution of portlandite was similar, with small clusters of platy crystals observed under the electron microscope. Samples A and D had an even distribution of small portlandite crystals throughout the matrix; the latter showing extensive portlandite development as a result of lengthy water storage. Samples B and C showed a similar pattern of abundant portlandite, although a slightly coarser texture was noted optically. While the distribution of crystals was generally even, there were occasional concentrations of larger crystals at the paste/aggregate interface. Concrete F revealed a similar distribution of portlandite to B and C, with occasional rims lining voids. Sample E exhibited the microstructure with the most diagnostic features: a coarse texture was evident with concentrations of larger crystals in microcracks, especially those at the paste/aggregate interface, and in air voids. Optical microscopy revealed that very small crystals of portlandite were abundant in zones around the microcracks and in areas with high concentrations of entrained air voids (represented by the dark zone in the central area of Plate 4). This is probably indicative of a locally higher water/cement ratio in these regions, perhaps due to capillary action drawing water preferentially into the microcracks, resulting in the development of a less dense paste. Portlandite rims around coarse aggregate particles are also associated with bleeding in concrete. In such circumstances films of water form at the aggregate surfaces, becoming sites of crystallisation, with movement of water occurring in bleed channels. This greater mobility of water, and thus ions, in zones around large aggregate particles may also help to explain the formation of hollow shells.

All of the samples showed a dense microstructure associated with the development of C-S-H gel. Although little difference could be detected in either the abundance or texture of the C-S-H in most of the concretes, sample E did show some indication of a coarser microstructure under the optical microscope, although electron microscopy revealed no obvious systematic difference in the thickness of the C-S-H shells formed around clinker grains.

Samples E and F showed more abundant ettringite than those cured at lower temperatures, its development being particularly extensive in the case of sample E; clusters of ettringite crystals

were obvious under the optical microscope both within the matrix and as larger needles and rods in microcracks, especially those at the paste/aggregate interface where they often occurred in association with portlandite (Plate 5), and in voids.

PLATE 5
Sample E: Optical micrograph (oblique polars, x200)

PLATE 6
Sample E: Scanning electron image

Microcracking

All of the concretes exhibited microcracking (both peripheral to, and to a lesser extent through, aggregate grains) which was visible under both the optical and electron microscope. In general terms, the width of the microcracks and the extent of their development increased with curing temperature from 5μm to 50μm in width, being particularly severe in the case of concrete E. In samples E and F the extensive network of microcracks was a prominent feature of the microstructure. These microcracks were commonly filled with hydrates (although this was not the case for the concretes cured at lower temperatures) which had a similar morphology in both cases - a crust-like layer with desiccation-type cracks which were either isolated or formed a network (Plate 6). Qualitative chemical analysis found the hydrate to contain calcium, aluminium and sulphur in ratios similar to those of ettringite, thus confirming the identification made by optical microscopy. Such ettringite-rich zones could also be associated with relatively high water levels in the paste leading to desiccation during sample preparation and preferred fracturing in these zones. The extensive microcracking of concrete E may be explained in part by the presence of poorly dispersed entrained air voids (Plate 4). During curing at such high temperatures this air would expand, with the result that regions of high air void concentration would suffer a greater build-up of stress which may be sufficiently high to overcome the strength of the matrix in the early stages of curing, thus leading to microcracking.

The formation of secondary ettringite may be a consequence of improved mobility of water (and thus ions) within the concrete due to the presence of microcracks which act as ideal moisture pathways. This crystallisation need not be the initial cause of microcracking (indeed a system of microcracks is evident, all be it not well developed, in concretes cured under ambient conditions) but may lead to their expansion and the development of a dense network of microcracks.

CONCLUSIONS

1. The samples manufactured at curing temperatures up to 46°C showed a similar microstructure to that seen at 20°C with only a limited coarsening of the fabric at 42°C and 46°C.

2. Concretes cured at higher temperatures exhibited a coarser microstructure than that typical of concrete cured at 20°C, particularly with respect to portlandite.
3. Microcracking was observed in all of the concretes, forming a prominent network in that cured at 85°C, and in the eighteen year old precast concrete.
4. The fissures within the most extensively microcracked concretes were characterised by hydrate infill, notably ettringite with some associated portlandite. Where microcracks occurred at the paste/aggregate interface, the ettringite occurred as a crust-like layer on the surface of coarse aggregate particles.
5. The presence of microcracks will increase moisture mobility within the concrete which may produce density gradients within the matrix leading to further microcracking. The domination of the matrix by a network of microcracks is conducive to the formation of secondary ettringite.

In order to improve our understanding of the processes which lead to microcracking, and the expansion which has been reported to occur in concretes cured at elevated temperatures, a number of samples have been prepared under controlled temperature and humidity regimes, between 20°C and 80°C. Following storage and ageing in a range of conditions, the microstructural development and performance of the concretes is being assessed.

ACKNOWLEDGEMENTS

The work reported here has been carried out as part of a research project funded by the Science and Engineering Research Council. The authors would like to acknowledge the assistance of BCA, Dow Mac Costain, and Scientifics (formerly British Rail Scientific Services).

REFERENCES

1. H.H.Patel, C.H.Bland and A.B.Poole, Departmental Working Paper, GR/J14936/1 (1993).
2. K.O.Kjellsen, R.J.Detwiler and O.E.Gjorv, Cem. Concr. Res., **20**, 308 (1990).
3. K.O.Kjellsen, R.J.Detwiler and O.E.Gjorv, Ibid., **20**, 927 (1990).
4. K.O.Kjellsen, R.J.Detwiler and O.E.Gjorv, Ibid., **21**, 179 (1991).
5. K.L.Scrivener, Ibid., **22**, 1224 (1992).
6. D.Heinz and U.Ludwig, Concr. Dur., K &B Mather Intl. Conf., Detroit,(SP100-105), Am. Concr. Inst., **2**, 2059 (1987).
7. G.Hempel, A.Bohmer and M.Otte, Concr. Precasting Plant and Tech., **5**, 75 (1992).
8. P.Tepponen and B.Kriksson, Nordic Concr. Res. Publ., **6**, 199 (1987).
9. A.Shayan and G.W.Quick, Adv. Cem. Res., **4** (16), 149 (1991/2).
10. R.E.Oberholster, H.Moore and J.H.B.Brand, 9th Intl. Conf. Alkali-Aggregate Reaction in Concrete, London, 739 (1992).
11. V.Johansen, N.Thalow and J.Skanly, Adv. Cem. Res., **5**(17), 23 (1993).
12. H.Siedel, S.Hempel and R.Hempel, Cem. Concr. Res., **20**, 453 (1993).
13. D.W.Hobbs and C.D.Lawrence, To be published.